(12) LEVEL II

AD-E300334

DNA 4543T

EFFECT OF MULTIPLE SCATTERING ON THE COMPTON RECOIL CURRENT

Mission Research Corporation
735 State Street
Santa Barbara, California 93101

February 1978

Topical Report for Period December 1977—February 1978

CONTRACT No. DNA 001-77-C-0135

THIS WORK SPONSORED BY THE DEFENSE NUCLEAR AGENCY
UNDER RDT&E RMSS CODE B323077464 R99QAXEA09172 H2590D.

Prepared for
Director
DEFENSE NUCLEAR AGENCY
Washington, D. C. 20305

Destroy this report when it is no longer needed. Do not return to sender.

PLEASE NOTIFY THE DEFENSE NUCLEAR AGENCY, ATTN: TISI, WASHINGTON, D.C. 20305, IF YOUR ADDRESS IS INCORRECT, IF YOU WISH TO BE DELETED FROM THE DISTRIBUTION LIST, OR IF THE ADDRESSEE IS NO LONGER EMPLOYED BY YOUR ORGANIZATION.

UNCLASSIFIED (12) DNA, SBIE

SECURITY CLASSIFICATION OF THIS PAGE (When Data Entered)

REPORT DOCUMENTATION PAGE

READ INSTRUCTIONS BEFORE COMPLETING FORM

1 REPORT NUMBER (19) DNA 5431, AD-E500 222	2 GOVT ACCESSION NO / 3 RECIPIENT'S CATALOG NUMBER
4 TITLE (and Subtitle) (6) EFFECT OF MULTIPLE SCATTERING ON THE COMPTON RECOIL CURRENT	5 TYPE OF REPORT & PERIOD COVERED (9) Topical Report, ~~for Period~~ December 1977—February 1978
	6 PERFORMING ORG. REPORT NUMBER (14) MRC-R-378
7 AUTHOR(s) (10) Conrad L. Longmire	8 CONTRACT OR GRANT NUMBER(s) (15) DNA 001-77-C-0135
9 PERFORMING ORGANIZATION NAME AND ADDRESS Mission Research Corporation 735 State Street Santa Barbara, California 93101	10 PROGRAM ELEMENT, PROJECT, TASK AREA & WORK UNIT NUMBERS Subtask R99QAXEA091-72
11 CONTROLLING OFFICE NAME AND ADDRESS Director Defense Nuclear Agency Washington, D.C. 20305	12 REPORT DATE (11) February 1978 / 13 NUMBER OF PAGES 52
14 MONITORING AGENCY NAME & ADDRESS (if different from Controlling Office)	15 SECURITY CLASS (of this report) UNCLASSIFIED / 15a DECLASSIFICATION/DOWNGRADING SCHEDULE

16 DISTRIBUTION STATEMENT (of this Report)

Approved for public release; distribution unlimited.

(12) 52 p. (16) R99QAXE (17) A091

17 DISTRIBUTION STATEMENT (of the abstract entered in Block 20, if different from Report)

18 SUPPLEMENTARY NOTES

This work sponsored by the Defense Nuclear Agency under RDT&E RMSS Code B323077464 R99QAXEA09172 H2590D.

19 KEY WORDS (Continue on reverse side if necessary and identify by block number)

Electromagnetic Pulse
Compton Current
Nuclear Explosions, Effects Of

20 ABSTRACT (Continue on reverse side if necessary and identify by block number)

This report explains the approximate method used in the CHAP EMP computer code for calculating the Compton current as affected by multiple scattering, and compares its results with those from more accurate Monte Carlo calculations. It is shown that the CHAP method provides good accuracy. Results computed by Sollfrey are also compared with the Monte Carlo results, and found to be less accurate than expected.

DD FORM 1 JAN 73 1473 EDITION OF 1 NOV 65 IS OBSOLETE

UNCLASSIFIED

SECURITY CLASSIFICATION OF THIS PAGE (When Data Entered)

406 548

78 08 23 017

PREFACE

Robert M. Hamilton constructed the computer codes and ran all of the problems presented in this report. William Wortman and Kenneth Smith independently verified the calculation of the initial slope of the transverse current.

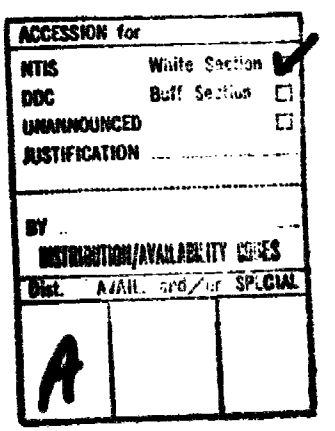

CONTENTS

ILLUSTRATIONS

SECTION 1
INTRODUCTION

The theory of the electromagnetic pulse (EMP) from high-altitude nuclear bursts was first developed in a series of lectures (Reference 1) given by this author at the Air Force Weapons Laboratory (AFWL) in January and February 1964. The essential part of the theory is that Compton recoil electrons, produced by the prompt gamma rays from the burst, are deflected by the geomagnetic field from the radial direction to a direction perpendicular to both the radial vector and the geomagnetic field. The transverse electric current so formed generates an outgoing EM wave which maintains coincidence with the gamma pulse and (therefore) with the Compton current; as a result of this coincidence, a large-amplitude pulse is built up, with duration (several tens of nanoseconds) determined by Compton electron dynamics. This short duration is in marked contrast to that of the EMP radiated by the radial Compton current, which is determined by the size of the source region (hundreds of kilometers) and leads to a smaller amplitude.

In Reference 1 the author derived the basic equation of the outgoing wave approximation,

$$\frac{1}{Z_0}\frac{\partial E_t}{\partial r} + \frac{1}{2}\sigma E_t = -\frac{1}{2}J_t \ . \qquad (0)$$

Here r is the radial coordinate (but with the gamma pulse treated as planar), E_t is the transverse electric field, J_t is the transverse Compton current density, σ is the electrical conductivity induced in the air, and $Z_0 = 377$ ohms is the impedance of space. The factors 1/2 occur because only outgoing

(and not ingoing) waves are generated with substantial amplitude. The equation says that, as r increases, E_t builds up in the direction of $-J_t$, but is attenuated by the conductivity. The retarded time t-r/c enters Equation 0 only as a parameter; that is, the equation deals with E_t and J_t at a constant retarded time. Sample Compton currents and conductivities were calculated in Reference 1, and the solution presented. A general discussion of the character of solutions was given, along with a discussion of the effect of diffraction, which explained why the solution of an equation along a single ray gives correct answers for a three-dimensional problem.

In largely independent work only slightly later than this author's, William Karzas and Richard Latter developed virtually the same theory (Reference 2). These authors chose to work in spherical coordinates, in which the derivative $\partial E_t/\partial r$ in Equation 0 is replaced by $\partial(rE_t)/r\partial r$, and they developed approximate analytical formulae for the Compton current, the conductivity, and the resulting field. There has been no important disagreement over the basic theory of the high-altitude EMP since 1964.

For a couple of years after the birth of the theory, Karzas and this author provided analytically-based estimates of the high-altitude EMP to military systems planners. Then John Erkkila of AFWL, working with consultation from Karzas, constructed the computer code HEMP which essentially mechanized the analytical models developed by Karzas and Latter. This code made it possible to produce EMP environment information easily for many burst heights, yields, and observer locations, and it was the principle source of such information for several years.

The analytical models contained quite a few approximations. In 1971, Jerry Longley and this author undertook, with support of the Defense Nuclear Agency (DNA), to develop a computer code with more accurate modeling of the basic phenomena. First, by solving the equations of motion of sample Compton electrons simultaneously with the solution of Maxwell's equations,

we obtained (Reference 3) the effect of the EMP fields on the Compton current (self consistency). Second, we developed a method, called the obliquity factor method, for treating the effect of multiple scattering of Compton electrons by air atoms (Reference 4). Third, we developed a method for treating the finite time required for secondary electrons to complete their ionization (Reference 5). The code which embodies these improvements, and others, is called CHAP (Reference 6). The AFWL codes CHEMP and HEMP-B employ the same methods, and most of the current high-altitude EMP environments are computed with one or another of these codes.

Recently (Reference 7), William Sollfrey has calculated the effect of multiple scattering on the Compton current by a new method developed by him, and has raised questions about the basis and the accuracy of the obliquity factor method.

In the present report we explain the basis of the obliquity factor method, and test its accuracy against Monte Carlo calculations. We shall see that it is quite accurate. It is, in fact, more accurate than we had expected.

We also compare with Sollfrey's calculations and find, to our disappointment, that his method does not apparently provide accurate answers for this difficult problem of multiple scattering. We are therefore left with having to rely on the Monte Carlo calculations for accuracy standards.

SECTION 2
PROBLEM DEFINITION

The prompt gamma rays from a nuclear burst are emitted in a few tens of nanoseconds. For a burst far above the atmosphere, the gamma rays at time t after the burst lie within a spherical shell of radius ct (c is the speed of light) and with thickness of the order of 10 meters. The downward going part of this shell begins to interact with the atmosphere at an altitude of about 50 km. By 30 km, where the gamma scattering length is about equal to the atmospheric scale height $h \approx 6.7$ km, of the order of one-half of the gammas have been scattered by the Compton scattering process. By 20 km, only about 1 percent of the gammas have not been scattered. The dominant source region for the high-altitude EMP lies between 20 and 40 km altitude.

The mean scattering angle θ of the gammas is of the order of 30 degrees. Hence in the interval before a second scattering of a gamma occurs it will fall behind the unscattered gammas by a distance $\approx \lambda(1-\cos\theta) \approx 0.13\ \lambda \approx 1$ km. The scattered gammas therefore occupy a much thicker shell than the unscattered gammas, and the flux of scattered gammas is very small compared with that of the unscattered gammas in the thin shell occupied by the latter. For the first hundred nanoseconds of the EMP, the previously scattered gammas can be ignored.

The motion of Compton recoil electrons is limited by their Larmor radius in the geomagnetic field, and by energy loss in the air, to distances of the order of 100 meters from their birth place. Over this distance one can, with little error, consider the gamma shell to be planar, the gammas

parallel, and the γ intensity constant in space at a given retarded time T,

$$T = t - \frac{z}{c} . \qquad (1)$$

Here we have used the Cartesian coordinate z instead of r as the (large) distance from the burst point. (Of course, once we have gone to Cartesian coordinates, we can choose the origin of z arbitrarily.) Thus over the region of space of interest in calculating the Compton current, we can regard the gamma flux F_γ as being a function of T alone,

$$F_\gamma = F_\gamma(T) . \qquad (2)$$

Since the air density and geomagnetic field are also very nearly constant over 100 meters, the Compton current density, the air conductivity, and the EMP fields are also, to good approximation, functions of the retarded time alone over the range of the Compton electrons. This approximation greatly simplifies the problem of calculating the Compton current and the EMP.

The EMP fields affect the motion of the Compton electrons. Thus for an accurate calculation it is necessary to solve Maxwell's equations for the fields simultaneously with the equations of motion of the Compton electrons. Since the combined problem of particles and fields is nonlinear, there is little hope of solving it accurately by analytical means for general cases; we are reduced to using numerical methods.

In considering numerical methods, we have to choose between dealing with particles or with a distribution function, i.e., between solving Newton's laws or the Boltzmann equation. In the Boltzmann equation treatment, the distribution function will be a function of four variables: T and the three components of electron momentum. The fine gridding of momentum space required for accurate solutions makes this method generally more time consuming than particle methods. (We do not want to rule out the possibility of inventing a clever method for reducing the number of grid points required.)

Turning to particle treatments, we think first of Monte Carlo methods, because of the phenomenon of scattering of the Compton electrons by air atoms, which must be included for an accurate solution. However, the random fluctuations in Monte Carlo calculations will falsify the high-frequency content of the calculated EMP unless very large numbers of electrons are processed. The computing time consumed makes the Monte Carlo method suitable only for infrequent checks on faster methods.

It can be estimated, and we shall later show, that scattering causes only about a 30 percent reduction of the peak Compton current at 30 km altitude, which is the center of the EMP source region and the place where the largest EMP is generated. Thus there is hope that an approximate method of including scattering could give answers accurate to, say, 10 percent, which would be adequate. To this end we invented the obliquity factor method. It includes the effect of electron scattering without use of random numbers.

SECTION 3
COMPTON SCATTERING

The Compton recoil electrons (Reference 8) are produced in collisions of the gamma rays with electrons in the air atoms. In such a collision, the gamma is scattered to angle θ from its original direction (see Figure 1), and the electron goes off at angle ψ. The initial and final gamma directions and the electron direction lie in a plane. The azimuthal angle of this plane, or, to be specific, of the scattered gammas, about the original gamma direction is denoted by ϕ. We neglect the effect of binding of the electrons in the atoms, which is believed to be small.

We shall use the convenient relativistic notation in which

$$\left.\begin{aligned} \gamma &= \text{photon energy}/mc^2 = \text{photon momentum}/mc \\ \varepsilon &= \text{electron total energy}/mc^2 \\ \vec{p} &= \text{electron momentum}/mc \end{aligned}\right\} \qquad (3)$$

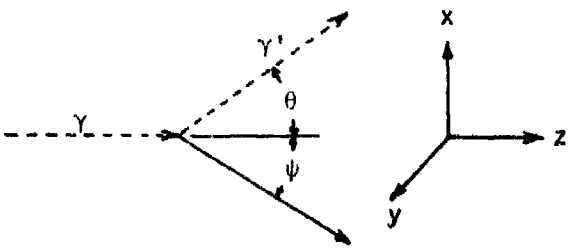

Figure 1. Geometry of Compton scattering.

Here m is the electron rest mass, and c the speed of light. From energy and momentum conservation one can determine the dependence of γ' and ϵ on γ and θ:

$$\gamma' = \frac{\gamma}{1 + \gamma\chi} \quad , \tag{4}$$

$$\epsilon = 1 + \gamma - \gamma' = 1 + \frac{\gamma^2\chi}{1 + \gamma\chi} \quad , \tag{5}$$

where

$$\chi \equiv 1 - \cos\theta \quad , \quad 0 \leq \chi \leq 2 \quad . \tag{6}$$

One also finds the z-component of electron momentum

$$p_z = \gamma - \gamma'\cos\theta = \gamma(1+\gamma)\frac{\chi}{1 + \gamma\chi} \quad . \tag{7}$$

The additional relativistic relations,

$$\epsilon = \sqrt{p^2 + 1} \quad , \tag{8}$$

$$\frac{v_z}{c} = \frac{p_z}{\epsilon} \quad \text{etc.} \quad , \tag{9}$$

are also useful. In Equation 9, v_z is the z-component of electron velocity; similar equations hold for the other components.

The probability of scattering to angle θ is given by the formula of Klein and Nishina. The differential cross section of an electron for scattering the gamma into solid angle $d\Omega$ at θ is

$$\sigma(\theta)d\Omega = \frac{r_0^2}{2} \frac{d\Omega}{(1+\gamma\chi)^2}\left[1 + (1-\chi)^2 + \frac{\gamma^2\chi}{1 + \gamma\chi}\right] \quad . \tag{10}$$

Here $r_0 = e^2/mc^2$ is the classical electron radius, where -e is the electron charge (cgs units). The element of solid angle is, after integrating over ϕ,

$$d\Omega = 2\pi \sin\theta d\theta = 2\pi d\chi \ . \tag{11}$$

The total scattering cross section per electron is obtained by integrating Equation 10 over χ, and is

$$\sigma_T = \pi r_0^2 T_1(\gamma) \ , \tag{12}$$

where

$$T_1(\gamma) = \frac{2(2+8\gamma+9\gamma^2+\gamma^3)}{\gamma^2(1+2\gamma)^2} - \frac{2+2\gamma-\gamma^2}{\gamma^3} \ln(1+2\gamma) \ . \tag{13}$$

For the gamma flux given by Equation 2, the total source density of Compton electrons is

$$S_T(T) = NZ\sigma_T F_\gamma(T) \ . \tag{14}$$

Here N is the density of air atoms and Z = 7.2 is the mean atomic number of air.

SECTION 4
THE BOLTZMANN EQUATION

We originally derived the obliquity factor method by considering particles rather than the distribution function. Since that derivation apparently left something to be desired in clarity, we shall derive it here from the Boltzmann equation. Let $f(\vec{r},\vec{p},t)$ be the density of Compton electrons in the six dimensional phase space of coordinate $\vec{r}$ and momentum $\vec{p}$. The six-dimensional velocity of the particles in phase space near the point $\vec{r},\vec{p}$ is $\dot{\vec{r}},\dot{\vec{p}}$, where the dots indicate time derivatives of the particle qunatities:

$$\dot{\vec{r}} = \vec{v} = \text{three dimensional particle velocity,} \tag{15}$$

$$\dot{\vec{p}} = \text{force on particle at } \vec{r},\vec{v} \text{ .} \tag{16}$$

Part of the force comes from the electric and magnetic fields. We shall also imagine that a resistive force acts on the Compton electrons, to account for their gradual loss of energy to other electrons in air atoms. The scattering of the Compton electrons by air atoms will be treated as a separate, scattering term in the Boltzmann equation.

The six-dimensional current of particles in phase space is $(\dot{\vec{r}},\dot{\vec{p}})f$, and the six-dimensional gradient operator is (∇_r,∇_p) where the subscripts indicate whether the three-dimensional gradient operates on coordinate or momentum space variables. The six-dimensional divergence of the six-dimensional particle current is

$$(\nabla_r,\nabla_p) \cdot \left[(\dot{\vec{r}},\dot{\vec{p}})f\right] = \nabla_r \cdot (\dot{\vec{r}}f) + \nabla_p \cdot (\dot{\vec{p}}f)$$

$$= \vec{v} \cdot \nabla_r f + \nabla_p \cdot (\dot{\vec{p}}f) \ . \qquad (17)$$

Here the order of ∇_r and $\vec{v}$ can be interchanged because $\vec{v}$ is a function of the momentum variables (see Equations 8 and 9), which are independent variables from $\vec{r}$. The order of ∇_p and $\dot{\vec{p}}$ cannot be interchanged because of the resistive force which depends on $\vec{p}$ in such a way that $\nabla_p \cdot \dot{\vec{p}} \neq 0$.

The conservation of particles is expressed by the Boltzmann equation,

$$\frac{\partial f}{\partial t} + \vec{v} \cdot \nabla_r f + \nabla_p \cdot (\dot{\vec{p}}f) = S + \int K(\vec{p},\vec{p}')f(\vec{p}')d^3p' \ . \qquad (18)$$

Here S is the source density of Compton electrons in Compton collisions, and the integral with K is the scattering operator, which takes particles out of momentum $\vec{p}'$ and places them at momentum $\vec{p}$.

It is important to realize that the Boltzmann equation is completely equivalent to Newton's laws of motion. If we start with an f which is a sum of delta functions, each singularity representing a point particle, and solve the equation forward in time, then the delta functions will be preserved and they will move exactly as particles would under Newton's laws. To make this work, the source S and the scattering operator have to be regarded as stochastic operators, which occassionally inject additional point particles or scatter point particles from one momentum to another. On the other hand, one can regard f as a continuous function expressing the probability of finding a particle near $\vec{r},\vec{p}$, or as the density of particles.

We have seen that it is a good approximation to treat the source S as depending on $\vec{r}$ and t only through the retarded time,

$$S = S(t - \frac{z}{c}, \vec{p}) = S(T, \vec{p}) \quad . \tag{19}$$

With this source, the Boltzmann equation and Maxwell's equations allow solutions which are functions of T alone. On substituting

$$f = f(t - \frac{z}{c}, \vec{p}) \quad , \tag{20}$$

into the Boltzmann equation we find

$$\frac{\partial}{\partial T}(1 - \frac{v_z}{c})f + \nabla_p \cdot (\dot{\vec{p}}f) = S + \int K f d^3p' \quad . \tag{21}$$

Here the factor $(1-v_z/c)$ can be placed on either side of the retarded time derivative. We can make this equation look more like a standard Boltzmann equation in momentum space by introducing a modified distribution function

$$F(T, \vec{p}) = (1 - \frac{v_z}{c})f \quad , \quad f = \frac{F}{(1 - \frac{v_z}{c})} \quad . \tag{22}$$

Then Equation 21 becomes

$$\frac{\partial F}{\partial T} + \nabla_p \cdot (\overset{\circ}{\vec{p}} F) = S(T, \vec{p}) + \int K^* F d^3p' \quad , \tag{23}$$

where

$$\overset{\circ}{\vec{p}} = \frac{1}{(1 - \frac{v_z}{c})} \frac{d\vec{p}}{dt} \quad , \tag{24}$$

$$K^* = K(\vec{p}, \vec{p}') \frac{1}{1 - \frac{v'_z}{c}} \quad . \tag{25}$$

Now from Equation 1 we find that if we move along with a particle,

$$dT = (1 - \frac{v_z}{c})dt \quad , \tag{26}$$

so that

$$\overset{\circ}{\vec{p}} = \frac{d\vec{p}}{dT} \quad . \tag{27}$$

The interpretation of K* is equally simple. The scattering kernel K contains a collision rate and an angular distribution. Equation 25 shows that the collision rate in retarded time is increased by the retarded-time factor $1/(1-v_z'/c)$. Particles that move forward with v_z close to c are acted upon by forces and scattering more quickly in retarded time, because the real time interval is longer for these particles than the retarded-time interval. Note, however that the source S does not acquire the retarded-time factor.

We can go immediately from Equation 23 to a completely equivalent set of point particles. We create particles according to the probability distribution in $S(T,\vec{p})$. The momenta of these particles change at the rate

$$\frac{d\vec{p}}{dT} = \frac{1}{1 - \frac{v_z}{c}} \times \text{usual forces} , \qquad (28)$$

and they scatter at a rate increased by a factor $1/(1-v_z/c)$ over the usual rate, but with the usual angular distribution. In adding up the current densities for these particles, we multiply the contribution of each particle by a factor $1/(1-v_z/c)$ because that factor occurs in the relation (22) between the true f and the modified F. This is the method used in CHAP, except that we also treat the scattering approximately, as we discuss later.

The physical explanation of the retarded-time factor appearing in the current contribution of each particle was given in Reference 3. It is that, for two Compton electrons <u>born</u> at places with z-coordinates differing by ΔZ_0 and having identical (but displaced) trajectories, the actual distance apart of these two particles at any given time is $\Delta Z = \Delta Z_0(1-v_z/c)$ as indicated in Figure 2. The density of <u>electrons</u> is therefore greater than the density of <u>births</u> by the retarded-time factor.

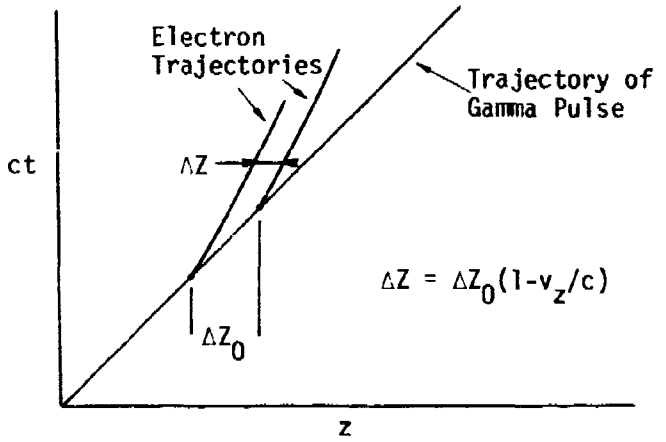

Figure 2. Explanation of retarded-time factor appearing in the current contribution of each particle. Relation between ΔZ and ΔZ_0 holds in the limit as $\Delta Z_0 \to 0$.

We hope this discussion of the retarded time equations will clear up any doubts for both those who prefer the Boltzmann approach and others who prefer the particle approach.

SECTION 5
INITIAL VALUE OF COMPTON CURRENT

For a delta-function pulse of gamma rays, we can calculate exactly the initial value of the radial Compton current. Also for the transverse Compton current, which starts from zero at T = 0, we can calculate exactly the initial rise rate. These two quantities are not affected by either energy loss or scattering.

The contribution of a given electron to the radial Compton current is proportional to

$$\delta J_z = \frac{v_z/c}{1 - v_z/c} = \frac{p_z}{\epsilon - p_z} = \gamma(1+\gamma)\chi \ . \tag{29}$$

Let us imagine a magnetic field B in the y-direction (see Figure 1), which will lead to a current in the x-direction. The contribution of a given electron to J_x is proportional to

$$\delta J_x = \frac{v_x/c}{1 - v_z/c} = \frac{p_x}{\epsilon - p_z} \ . \tag{30}$$

The average of this expression over the Klein-Nishina distribution vanishes by symmetry. The derivative with respect to retarded time is

$$\dot{\delta J}_x = \frac{\dot{p}_x}{\epsilon - p_z} + \frac{p_x \dot{p}_z}{(\epsilon - p_z)^2} \ . \tag{31}$$

The result of the resistive (energy loss) force and of scattering would be

to keep the distribution symmetrical in the angle ϕ about the axis formed by the original gamma ray direction. Therefore they do not contribute to the average of $\overset{\circ}{\delta J}_x$. Only the magnetic force will contribute. (we assume here that there is no electric field, although we could also calculate its effect.) For the magnetic force,

$$\left.\begin{aligned} \overset{\circ}{p}_x &= \frac{eB}{m}\frac{v_z/c}{1 - v_z/c} = \frac{eB}{m}\frac{p_z}{\varepsilon - p_z} , \\ \overset{\circ}{p}_z &= -\frac{eB}{m}\frac{v_x/c}{1 - v_z/c} = -\frac{eB}{m}\frac{p_x}{\varepsilon - p_z} . \end{aligned}\right\} \tag{32}$$

We then calculate

$$\overset{\circ}{\delta J}_x = \frac{eB}{m}\left[\frac{p_z}{(\varepsilon-p_z)^2} - \frac{p_x^2}{(\varepsilon-p_z)^3}\right] . \tag{33}$$

Now when averaging over the angle ϕ,

$$\begin{aligned} \mathrm{av}(p_x^2) &= \mathrm{av}(p_y^2) = \frac{1}{2}\,\mathrm{av}(p_x^2+p_y^2) \\ &= \frac{1}{2}\,\mathrm{av}(\varepsilon^2-1-p_z^2) . \end{aligned} \tag{34}$$

Thus when averaged over ϕ, we obtain

$$\begin{aligned} \overset{\circ}{\delta J}_x &= \frac{eB}{m}\frac{1}{2}\frac{1 - (\varepsilon-p_z)^2}{(\varepsilon-p_z)^3} \\ &= \frac{eB}{m}\frac{1}{2}\left[(1+\gamma\chi)^3 - (1+\gamma\chi)\right] . \end{aligned} \tag{35}$$

To find the initial value of J_z and $\overset{\circ}{J}_x$, we have to average Equations 29 and 35 over the Klein-Nishina distribution in χ, Equations 10 and 11. This averaging is straight forward, if a little tedious. The results are, in MKS units:

$$J_z(0) = - N_0 ec T_z(\gamma)/T_1(\gamma) \ , \tag{36}$$

$$\mathring{J}_x(0) = -N_0 ec \left(\frac{eB}{m}\right) T_x(\gamma)/T_1(\gamma) \ . \tag{37}$$

Here N_0 is the total number of Compton electrons produced per unit volume, T_1 is given by Equation 13, and

$$T_z = (1+\gamma)\left[2 + \frac{2\gamma}{(1+2\gamma)^2} - \frac{6 + 2\gamma}{\gamma^2} + \frac{3 + 4\gamma - \gamma^2}{\gamma^3} \ln(1+2\gamma)\right] , \tag{38}$$

$$T_x = \frac{(1+2\gamma)^2}{3} + \frac{1 + \gamma}{\gamma(1+2\gamma)} + \frac{1}{\gamma^2} - \frac{1 + 2\gamma}{2\gamma^3} \ln(1+2\gamma) \ . \tag{39}$$

For comparison with later numerical calculations we record here values for gamma rays of energy 1.6 MeV and a magnetic field of 0.6 Gauss = 6×10^{-5} Weber/m^2:

$$- J_z(0)/(N_0 ec) = 7.70 \ , \tag{40}$$

$$-\mathring{J}_x(0)/(N_0 ec) = 26.54 \frac{eB}{m} = 2.80 \times 10^8/\text{sec} \ . \tag{41}$$

To obtain the results (36) and (37) in cgs Gaussian units, replace ec by e, and eB/m by eB/mc.

For a given flux of gammas, N_0 is itself proportional to T_1, so that J_z and $\mathring{J}_x$ are proportional to T_z and T_x. Graphs of these quantities versus gamma energy are given in Figure 3.

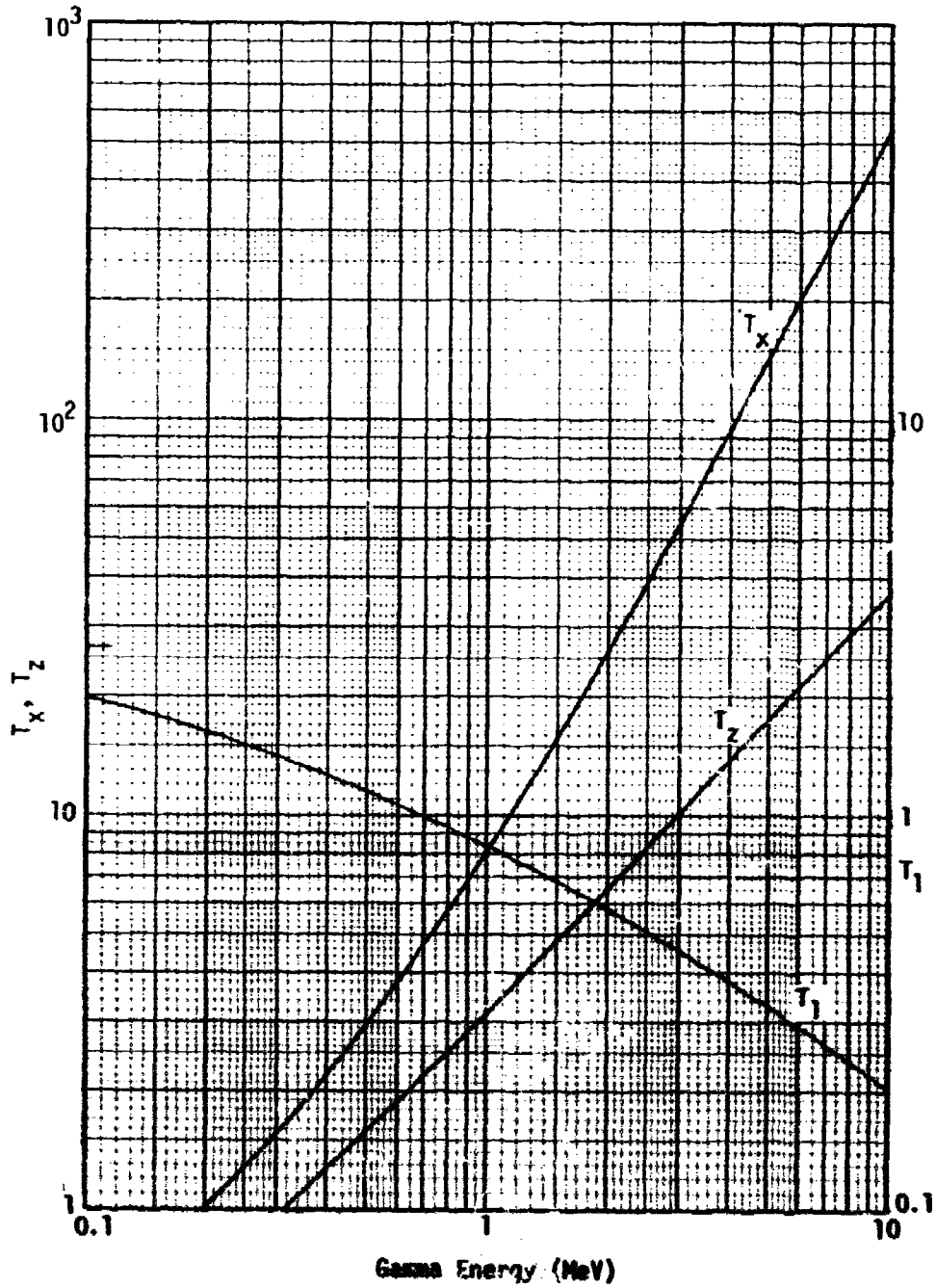

Figure 3. The quantities T_1, T_x, and T_z, as functions of gamma energy.

SECTION 6
ENERGY LOSS

For energy loss by the Compton electrons we use Bethe's formula (Reference 9). The mean change of energy dW per track length ds is

$$-\frac{1}{mc^2}\frac{dW}{ds} = 2\pi NZr_0^2\frac{\varepsilon^2}{p^2}[1] \quad . \tag{42}$$

Here N is the density of atoms of atomic number Z, r_0 is again the classical electron radius, and

$$[1] = \ell n\left[\frac{(mc^2)^2(\varepsilon-1)p^2}{2I^2}\right] - \left(\frac{2}{\varepsilon}-\frac{1}{\varepsilon^2}\right)\ell n2 + \frac{1}{\varepsilon^2}+\frac{1}{8}\left(1-\frac{1}{\varepsilon}\right)^2 \quad . \tag{43}$$

In this equation, I is the mean excitation potential, given in Reference 9 for various elements. For air and aluminum:

$$\begin{aligned} &\text{air:}\quad Z = 7.2 \quad , \quad I = 80.5 \text{ eV} \ , \\ &\text{A}\ell\text{:}\quad Z = 13 \quad , \quad I = 150 \text{ eV} \ . \end{aligned} \tag{44}$$

To save computational time, we approximate [1] by

$$[1] \approx 2\ell n\left(\frac{mc^2}{I}\right) + 3.42\ell n(p) - 1.71 \ , \tag{45}$$

$$\approx 15.80 + 3.42\ell n(p) \text{ for air} \ , \tag{46}$$

$$\approx 14.57 + 3.42\ell n(p) \text{ for A}\ell \ . \tag{47}$$

This approximation is accurate to 1 percent for electron kinetic energies between 25 keV and 5 MeV.

In the CHAP method we imagine that a steady force equal to dW/ds acts on the Compton electron, in the direction opposite to its velocity. Thus the energy of the electron decreases gradually at the correct average rate. This treatment ignores the fact that the energy loss occurs in steps of fluctuating magnitude. The probability distribution of energy losses w is given approximately by

$$P(w)dw \approx \frac{2w_0}{} \frac{dw}{w_0^2 + w^2} , \tag{48}$$

where w_0 is of the order of 10 eV. The average energy loss per inelastic collision is

$$\bar{w} \approx \frac{2w_0}{} \ln\left(\frac{W}{2w_0}\right) ,$$

$$\approx 60 \text{ eV for } W = 1 \text{ MeV} . \tag{49}$$

Thus the average step is very small compared with the energies W of the Compton electrons. However, since the integral of wP(w) gives a logarithm, roughly equal amounts of energy are lost in each decade in w; e.g., about 1/5 of the energy of a 1 MeV electron is lost in collisions that lose energy between 50 and 500 keV. Thus large energy losses are not totally negligible. We shall see, however, that at the center of the high altitude EMP source region (altitude ≈ 30 km), energy loss has only a small effect on the peak Compton current. It is unlikely that fluctuations in energy loss could cause changes in the peak current of more than a few percent.

In CHAP, ion pairs are created at the rate of one ion pair per 85 eV lost by the Compton electron. Secondary ionization then proceeds at the rate given in Reference 5, until there is one ion pair per 34 eV lost by the Compton electron.

SECTION 7
COULOMB SCATTERING

The differential cross section of a nucleus of charge Ze for scattering an electron into angular interval $d\theta$ at angle θ from its original direction is (Reference 9)

$$d\sigma = 4Z^2 r_0^2 \frac{\epsilon^2}{p^4} \frac{2\pi \sin\theta d\theta}{q^4} \quad . \tag{50}$$

Here q is proportional to the momentum change,

$$q = 2\sin\left(\frac{\theta}{2}\right) \qquad (0 \leq q \leq 2)$$

$$\approx \theta \text{ for } \theta << 1 \quad . \tag{51}$$

Note that the differential solid angle can be expressed in terms of q,

$$dq^2 = 2qdq = 4\sin\left(\frac{\theta}{2}\right)\cos\left(\frac{\theta}{2}\right)d\theta = 2\sin\theta d\theta \quad . \tag{52}$$

Thus

$$d\sigma = 4\pi Z^2 r_0^2 \frac{\epsilon^2}{p^4} \frac{dq^2}{q^4} \quad . \tag{53}$$

The total cross section, obtained by integrating over q, is infinite, since even distant collisions lead to some scattering for a pure Coulomb potential. However, screening of the nucleus by the atomic electrons reduces the scattering for large impact parameters. A good way to take into account the effect of the screening is to make the replacement

$$\frac{1}{q^2} \to \frac{1}{a^2 + q^2} \quad , \tag{54}$$

where a is effectively the minimum angle of scattering. Moliere (Reference 10) found a good fit to the scattering from the Thomas-Fermi atom by adding three terms of this form with different a's and different coefficients replacing unity in the numerator. We have picked a single value of a which gives the same result as Moliere's formulae for the following problem (which will be used in the next section).

We wish to find the integral over the differential cross section of the quantity

$$1 - \cos\theta = 2\sin^2\left(\frac{\theta}{2}\right) \approx \frac{1}{2} q^2 \quad . \tag{55}$$

This integral is

$$\int (1-\cos\theta)d\sigma = 4\pi Z^2 r_0^2 \frac{\epsilon^2}{p^4} \frac{1}{2} \int_0^2 \frac{q^2 dq^2}{(a^2+q^2)^2}$$

$$= 4\pi Z^2 r_0^2 \frac{\epsilon^2}{p^4} \frac{1}{2} \left[\ln\left(1 + \frac{4}{a^2}\right) - \frac{1}{1 + \frac{a^2}{4}} \right]. \tag{56}$$

In the cases of interest to us, $a^2/4$ will be very small compared with unity, so that we can approximate

$$\frac{1}{2}\left[\ln\left(1 + \frac{4}{a^2}\right) - \frac{1}{1 + \frac{a^2}{4}} \right] \approx \ln\left(\frac{2}{a}\right) - \frac{1}{2} = \ln \frac{1.213}{a} \quad . \tag{57}$$

Using Moliere's formulae, one can again do the integral of (1-cosθ), with considerably more work. The result is

$$\int (1-\cos\theta)d\sigma = 4\pi Z^2 r_0^2 \frac{\epsilon^2}{p^4} \ln\left(\frac{102\ p}{Z^{1/3}}\right) \quad . \tag{58}$$

(The number 102 inside the logarithm here replaces $137 = \hbar c/e^2$ in less accurate calculations of Coulomb scattering.) Comparing the Moliere result with Equations 56 and 57, we see that they will agree if we choose

$$a = \frac{Z^{1/3}}{84\ p} \quad . \tag{59}$$

We shall use the Moliere result (58) directly in the obliquity factor method drived in the next section. We have also used the differential cross section (53), with the replacement (54) and with a given by (59), to construct a Monte Carlo code for the purpose of testing the accuracy of the obliquity factor method. That code will be described in another report.

One often sees formulae like Equations 53 and 58 with Z^2 replaced by $Z(Z+1)$, for the alleged purpose of including the effect of scattering by the atomic electrons. This procedure may be approximately correct for the larger angle scattering (although it neglects the reduced-mass correction), but it can hardly be correct for the small angle scattering, where the atomic electrons are already taken into account in the screening. Possibly some form like $Z(Z + \frac{1}{2})$ might be appropriate. Since the correct procedure is apparently unknown, we leave the factor Z^2 in place.

SECTION 8
THE OBLIQUITY FACTOR

In Section 4 we derived the modified Boltzmann Equation 23 in retarded time and momentum space. This equation conserves particles in momentum space (whereas Equation 21 does not) and is directly equivalent to a set of particles whose accelerations and collision rates are modified by the retarded time factor. This equivalence is exact if the scattering operator is regarded as stochastic. We now derive an approximate, non-stochastic way of handling the scattering of the Compton electrons.

We consider first the case in which there are no forces (and no energy loss) and only scattering is acting. Then Equation 23 becomes

$$\frac{\partial}{\partial T} F(\vec{p}) = \int K(\vec{p},\vec{p}') \frac{F(\vec{p}')}{1 - v_z'/c} d^3p' \quad . \tag{60}$$

If we start with a particle with momentum $\vec{p}_0$, then F is initially a delta function

$$F_0(\vec{p}) = \delta(\vec{p}-\vec{p}_0) \quad .$$

As time goes on, $F(\vec{p})$ will spread out in angle around $\vec{p}_0$, but with no change in the magnitude $p = p_0$. The initial angular spread will be small because the scattering is predominantly small-angle. Therefore the factor $(1-v_z'/c)$ will vary only little over the distribution $F(\vec{p}')$ at early times, and may be replaced by its average value over that distribution. We thus write

$$\frac{\partial}{\partial T} F(\vec{p}) = \frac{1}{1 - \bar{v}_z/c} \int K(\vec{p},\vec{p}') F(\vec{p}') d^3p' \ , \qquad (61)$$

where the average $\bar{v}_z$ is a function of T but is independent of $\vec{p}$ and $\vec{p}'$.

In this approximation the central angle of the distribution does not change from the angle of $\vec{p}_0$. Let us calculate the rate of change of the quantity μ defined by

$$\mu \equiv \int \cos\alpha F(\vec{p}) d^3p \ , \qquad (62)$$

where α is the angle between $\vec{p}$ and $\vec{p}_0$. Multiplying Equation 61 by $\cos\alpha$ and integrating over $\vec{p}$, we find

$$\frac{d\mu}{dT} = \frac{1}{1 - \bar{v}_z/c} \iint \cos\alpha K(\vec{p},\vec{p}') F(\vec{p}') d^3p' d^3p \ . \qquad (63)$$

In the integral over $\vec{p}$, which we do first, we can choose $\vec{p}'$ as the axis of spherical coordinates. Then

$$\cos\alpha = \cos\theta\cos\beta - \sin\theta\sin\beta\cos\phi \ , \qquad (64)$$

where the angles are defined by Figure 4. Since K is a function only of the scattering angle θ and not of ϕ, the second term on the right in Equation 64 gives no contribution, and we have

$$\frac{d\mu}{dT} = \frac{1}{1 - \bar{v}_z/c} \int \cos\beta F(\vec{p}') d^3p' \int \cos\theta K(\theta) 2\pi \sin\theta d\theta \ . \qquad (65)$$

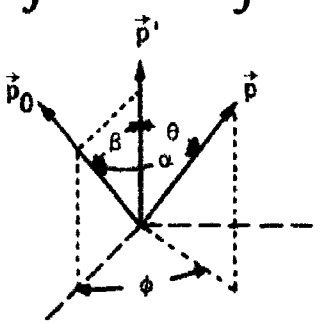

Figure 4. Angles for integration of Equation 63.

In these variables, the second integral is independent of $\vec{p}'$ and the first integral is μ. Thus

$$\frac{d\mu}{dT} = \frac{\mu}{1 - \bar{v}_z/c} \int \cos\theta K(\theta) 2\pi \sin\theta d\theta \ . \tag{66}$$

Now the scattering operator K removes particles from $\theta = 0$ (i.e., it contains a term $-\delta(\theta)$), and puts them at other angles $\theta > 0$. Since it conserves particles, we have

$$\int K(\theta) 2\pi \sin\theta d\theta = 0 \ . \tag{67}$$

We can therefore write Equation 66 as

$$\frac{d\mu}{dT} = - \frac{\mu}{1 - \bar{v}_z/c} \int (1-\cos\theta) K(\theta) 2\pi \sin\theta d\theta \ . \tag{68}$$

Since $1-\cos\theta$ vanishes at $\theta = 0$, the delta-function part of $K(\theta)$ gives no contribution to this integral, and K can be replaced by the differential scattering cross section of Section 7, multiplied by Nv to give a scattering rate. We thus obtain, from Equation 58, and noting that

$$v = c \frac{p}{\epsilon} \ , \tag{69}$$

the result,

$$\frac{1}{c} \frac{d}{dT} \ln\mu = - \frac{1}{1 - \bar{v}_z/c} 4\pi N Z^2 r_0^2 \frac{\epsilon}{p^3} \ln\left(\frac{102\ p}{Z^{1/3}}\right) \ . \tag{70}$$

A group of particles starting out with velocity

$$\vec{v}_0 = c \frac{\vec{p}}{\epsilon} \ , \tag{71}$$

will have an average velocity, as a result of scattering,

$$\vec{v} = \vec{v}_0 \mu \ . \tag{72}$$

This reduction in velocity affects the current densities and the relation between real time t and retarded time T for this group of particles. It

does not affect the ionization rate directly, which depends only on the magnitude of the momentum.

Let us now turn on the electromagnetic and resistive forces. Now the magnetic force rotates all of the momenta in the slightly-spread distribution (resulting from scattering) about the magnetic field axis; this changes the central angle of the distribution, but does not affect the angular spread μ. The resistive force reduces the magnitudes of all the momenta, but also does not affect μ directly. The electric force changes the components of all the momenta in the direction of the electric field; this changes both the central momentum and the angular spread, as explained in References 3 and 4.

We thus arrive at the obliquity factor method. It assigns a central momentum $\vec{p}$ to each particle, which is the momentum it would have in the absence of scattering. Associated with $\vec{p}$ in the usual way are the total energy ε and the central velocity $\vec{v}$. The equation of motion in retarded time is

$$\frac{d\vec{p}}{dT} = \frac{1}{1 - \frac{v_z}{c}\mu} \times \text{usual forces} \ . \tag{73}$$

The equation for μ is Equation 70 (when $E = 0$) with

$$\bar{v}_z = v_z \mu \ . \tag{74}$$

The contribution of a particle to the current density is proportional to

$$\delta\vec{J} = \frac{\frac{\vec{v}}{c}\mu}{1 - \frac{v_z}{c}\mu} = \frac{\vec{p}\mu}{\varepsilon - p_z\mu} \ . \tag{75}$$

Since μ starts from unity at $T = 0$, it can be seen that scattering does not affect the initial value of J_z, and that it does not affect the initial value of dJ_x/dT (for a magnetic field in the y-direction).

To the extent that scattering is dominated by small angle scattering, it is clear that the obliquity factor method should be asymptotically correct at early times, i.e., it should give the first order effect of scattering correctly. High accuracy at late times is not expected a priori, but we shall see what we get in the next section.

In earlier discussions of the obliquity factor method we used, instead of μ,

$$\eta = 1/\mu \quad , \quad \ell n\eta = - \ell n\mu \ . \tag{76}$$

The equation for η is therefore

$$\frac{1}{c}\frac{d\eta}{d\tau} = \eta \times \text{RHS} \ , \tag{77}$$

where RHS is the negative of the right-hand side of Equation 70. In our early work we dropped the factor η on the right in Equation 77, on the grounds that the model is valid only when η is not far from unity. This method, without the factor η, is called the "old method," whereas Equations 70 and 77 are called the "new method." We shall compare their relative accuracies in the next section.

SECTION 9
COMPARISON OF RESULTS

To test the accuracy of the CHAP method of computing Compton current, we shall compare its results with those from Monte Carlo calculations. In another report we shall describe two types of Monte Carlo calculations of different complexity. The simpler calculation treats all scattering as small-angle, using a Gaussian angular distribution of scattered particles; the width of the Gaussian is determined from the total scattering. The more sophisticated calculation divides the scattering into a small-angle part and another part not limited to small angles. The small angle part is assigned a Gaussian distribution, whereas the large angle part is given the screened Coulomb distribution. The sophisticated calculation is considerably more time consuming. We have used both methods to calculate the transmission of monoenergetic electrons through aluminum foils of various thicknesses, and have compared the results with the experimental data of Marshall and Ward (Reference 11). The results are shown in Figure 5. The two Monte Carlo methods give ranges, for a given transmitted fraction, which differ by not more than about 5 percent. The experimental results are very close to the Monte Carlo results for small foil thickness, but show ranges up to 10 percent larger for large thickness (low transmissions). We do not know what the absolute accuracy of the experimental data is, as Reference 11 gives no assessment of probable error. Spread in energy of the incident electrons would make the tails of the experimental curves extend to longer ranges. In addition, crystaline effects in the aluminum foils are not accounted for in the theory of multiple scattering, which assumes that the scattering atoms are randomly placed. This effect would not be present in air. Altogether,

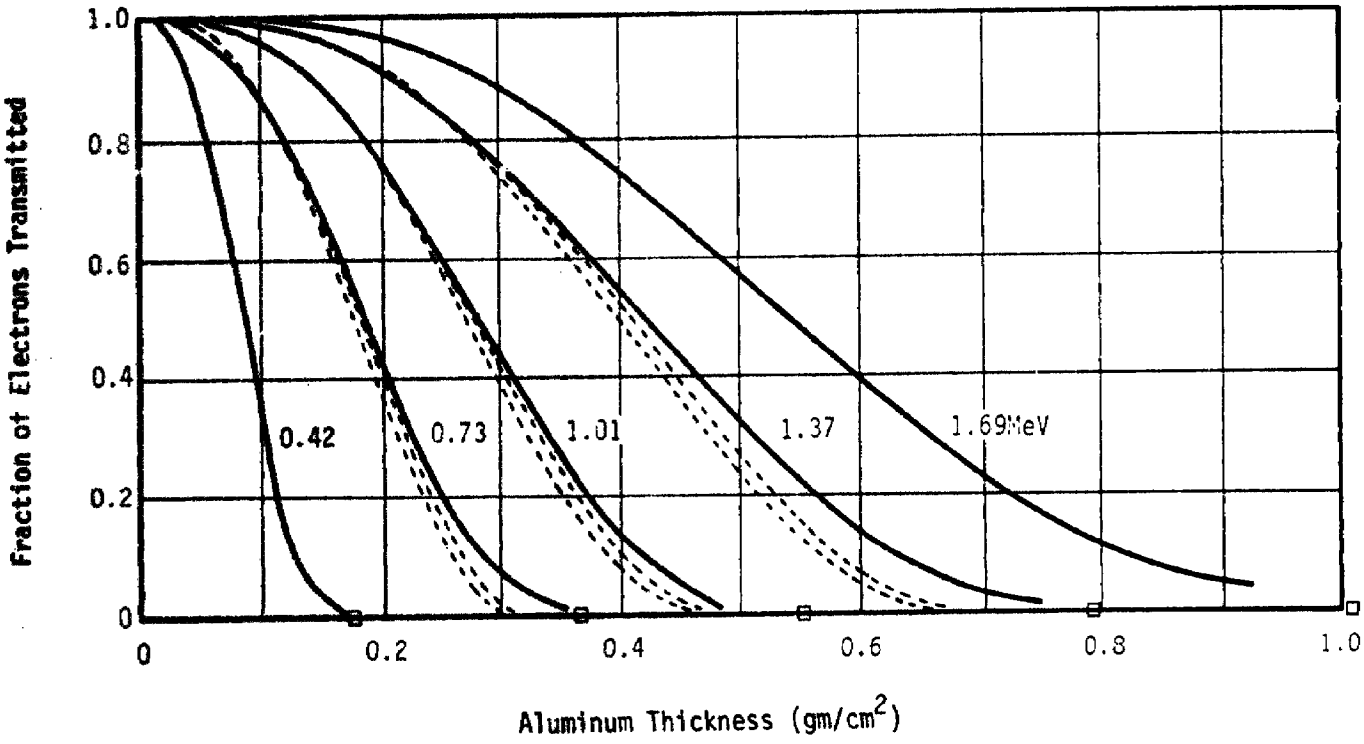

Figure 5. Transmission of energetic electrons through Aluminum foils. Solid curves, data of Marshall and Ward. Dashed curves, Monte Carlo results. Dashed curve nearest solid curve is from the more sophisticated Monte Carlo in all cases. Squares, calculated extreme ranges.

the agreement is quite good, and we shall assume that the sophisticated Monte Carlo represents the correct effects of multiple scattering and energy loss. Since the simple Monte Carlo gives results differing by only a few percent and is considerably faster, we have used it to compare with the CHAP method.

All of the calculations were done with gamma rays of energy 1.6 MeV and for a transverse magnetic field of 0.6 Gauss. No EMP fields (self consistency) were included. Two altitudes were used:

altitude = 30 km, air density = 1.84×10^{-5} gm/cm^3;

altitude = 20 km, air density = 8.89×10^{-5} gm/cm^3.

Figure 6 shows transverse currents at 30 km altitude. The curve labeled VAC was computed by the CHAP equations but with the resistive force and scattering set equal to zero, i.e., it represents the case of zero air density. For the curve EL, the resistive force was turned on, but scattering was omitted. The curve labeled CHAP includes both effects. We see that scattering causes a larger effect than energy loss. The curve labeled MC is the Monte Carlo result. It is a few percent larger than the CHAP result at times of several nanoseconds. We shall see later (Figure 9) that the ionization rate is also a little larger from the Monte Carlo calculations; these two errors tend to cancel in determining the peak electric field, which is proportional to J_x/σ (σ is the conductivity). We see that all the curves approach the theoretical slope at early times, although scattering causes departure quite early in retarded time. The time step used in the calculations was 0.3 nanoseconds. For the most energetic electrons, the real time step is about 27 times longer. We see that the difference between the old and new obliquity factor treatments is small over the time frame presented, with the old method being a little closer to the Monte Carlo results.

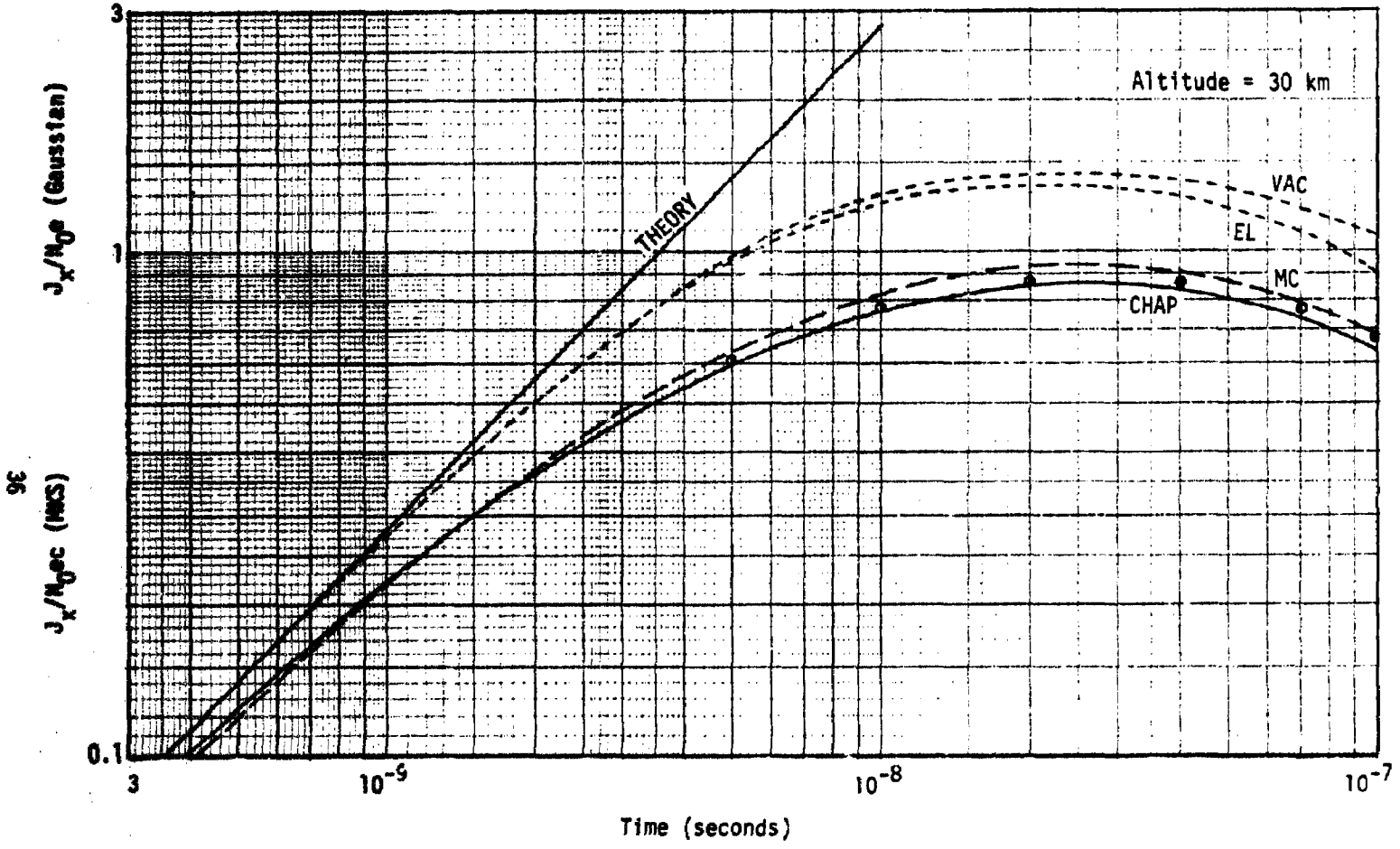

Figure 6. Transverse current for E_γ = 1.6 MeV, B_y = 0.6 Gauss, altitude = 30 km. Curve labels indicate: THEORY, theoretical slope; VAC, zero air density; EL, energy loss included, but no scattering; MC, Monte Carlo; CHAP, new obliquity factor method. Circles are points from old method.

Figure 7 shows the transverse current at 20 km altitude. Here the Monte Carlo and CHAP results are very close together at times of interest. The old method is substantially too large after 2×10^{-8} second, as expected since it underestimates the scattering when μ is small (or η is large). However, this error would not affect the peak EMP.

The transverse currents at both altitudes are shown in a linear plot in Figure 8.

Figure 9 gives the ionization rates at the two altitudes, based on instantaneous production of one ion pair per 34 eV lost by the Compton electron. The CHAP code takes account of the time lag for secondary ionization, but we have omitted this lag here to better compare the calculations. (Including the lag would bring the Monte Carlo and CHAP results a little closer together, since both curves start from the same initial value.) At 30 km altitude, the Monte Carlo result is larger than the CHAP result by a little more than the error in the transverse current. The computed peak EMP from CHAP will therefore be a few percent too large.

Figure 10 shows the radial current at both altitudes. The difference between the Monte Carlo and CHAP results is maximum for this component. Fortunately, the radial current has practically no effect on the EMP except at points very close to the burst, where EMP is usually not of primary concern. The radial currents all start from the theoretical initial value.

As a final check on the accuracy of our calculations, we compare in Figure 11 our CHAP results with some older Monte Carlo calculations of Knutson and Morgan (Reference 12). These calculations were made for 20-km altitude, but with slightly different E_γ and β from those we have been using. CHAP was run with these revised values. Figure 11 shows quite good agreement between CHAP and the Knutson-Morgan Monte Carlo. Comparing Figure 11 with Figure 8 (for 20-km altitude), we see that the relation of the Monte

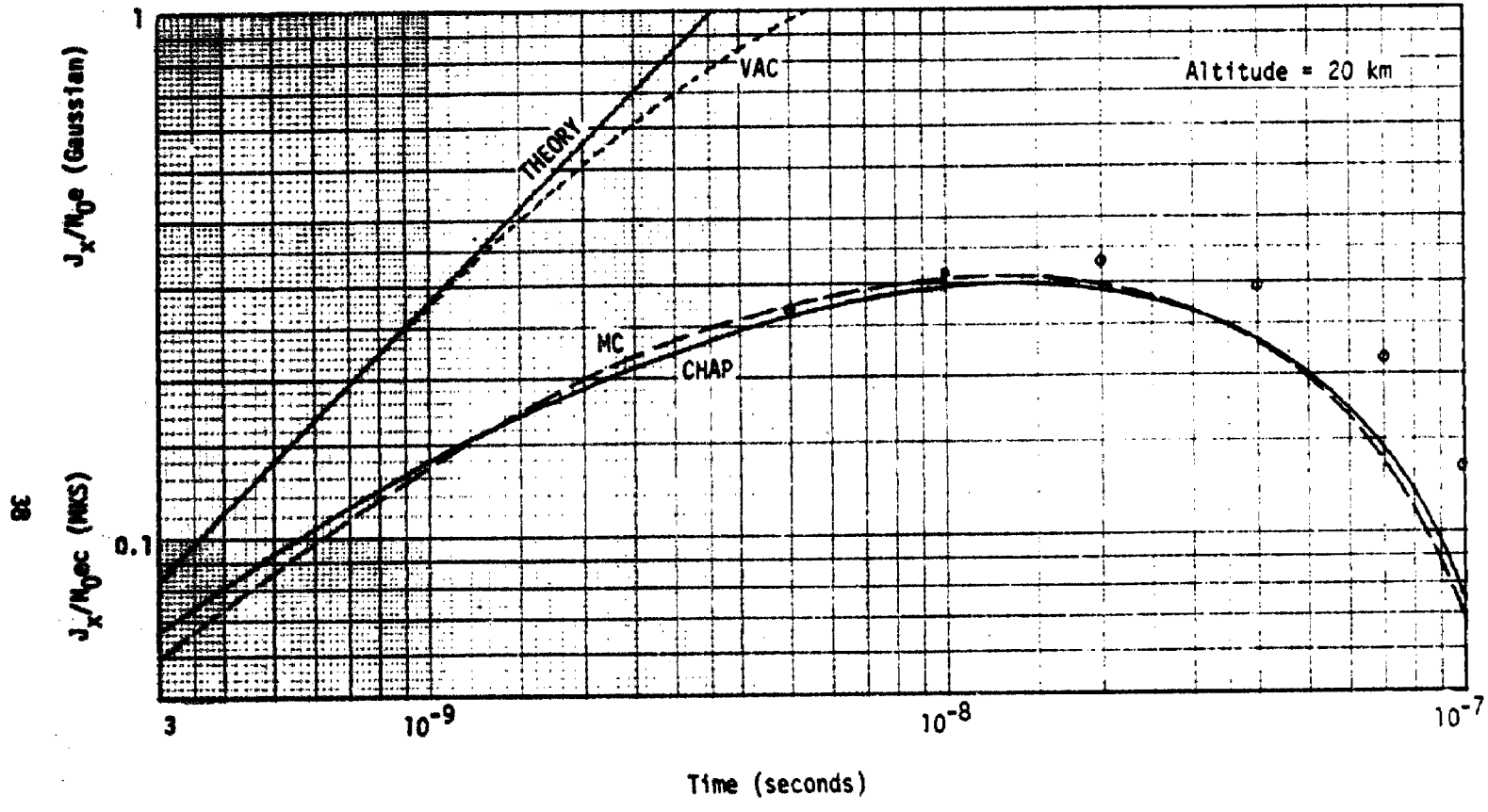

Figure 7. Transverse current for E_γ = 1.6 MeV, B_γ = 0.6 Gauss, altitude = 20 km. Curve labels indicate: THEORY, theoretical slope; VAC, zero air density; MC, Monte Carlo; CHAP, new obliquity factor method. Circles are points from old method.

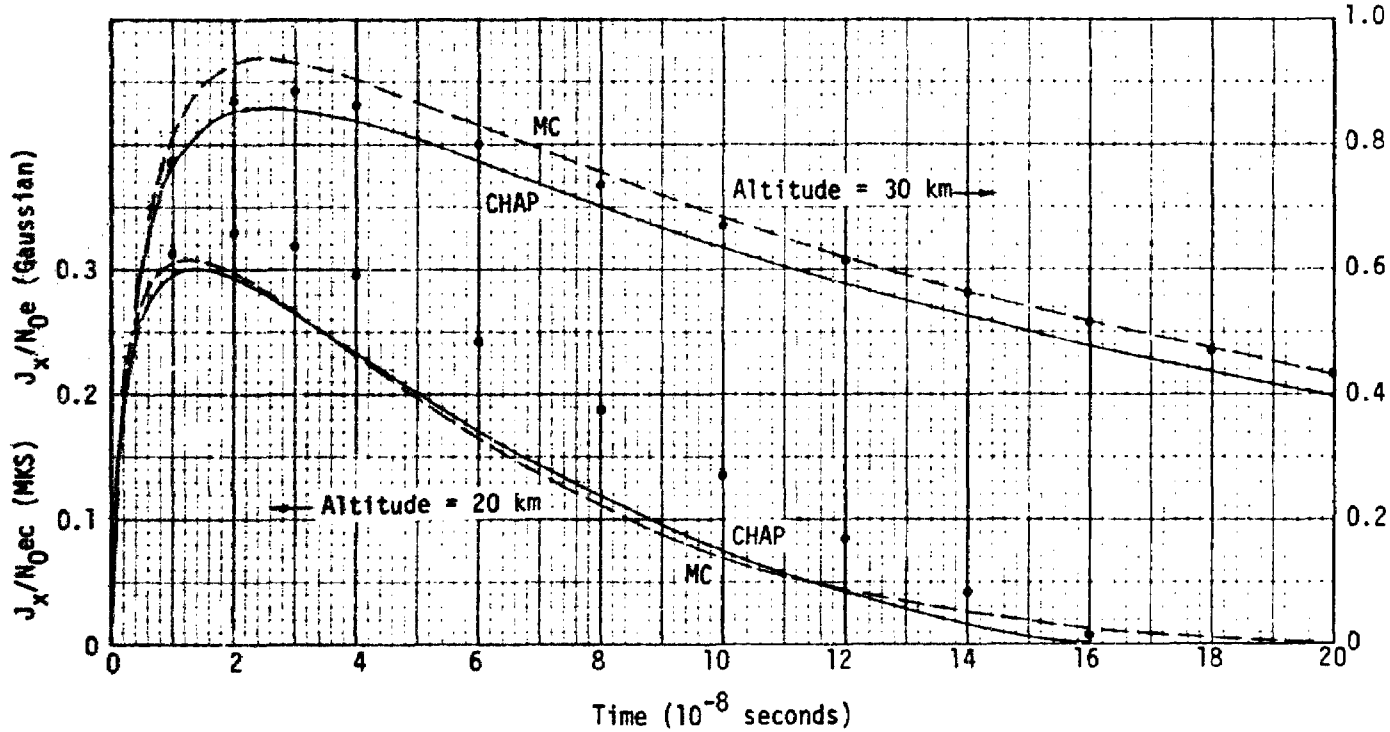

Figure 8. Transverse current for E_γ = 1.6 MeV, B_y = 0.6 Gauss. Curve labels indicate: MC, Monte Carlo; CHAP, new obliquity factor method. Circles are points from old method.

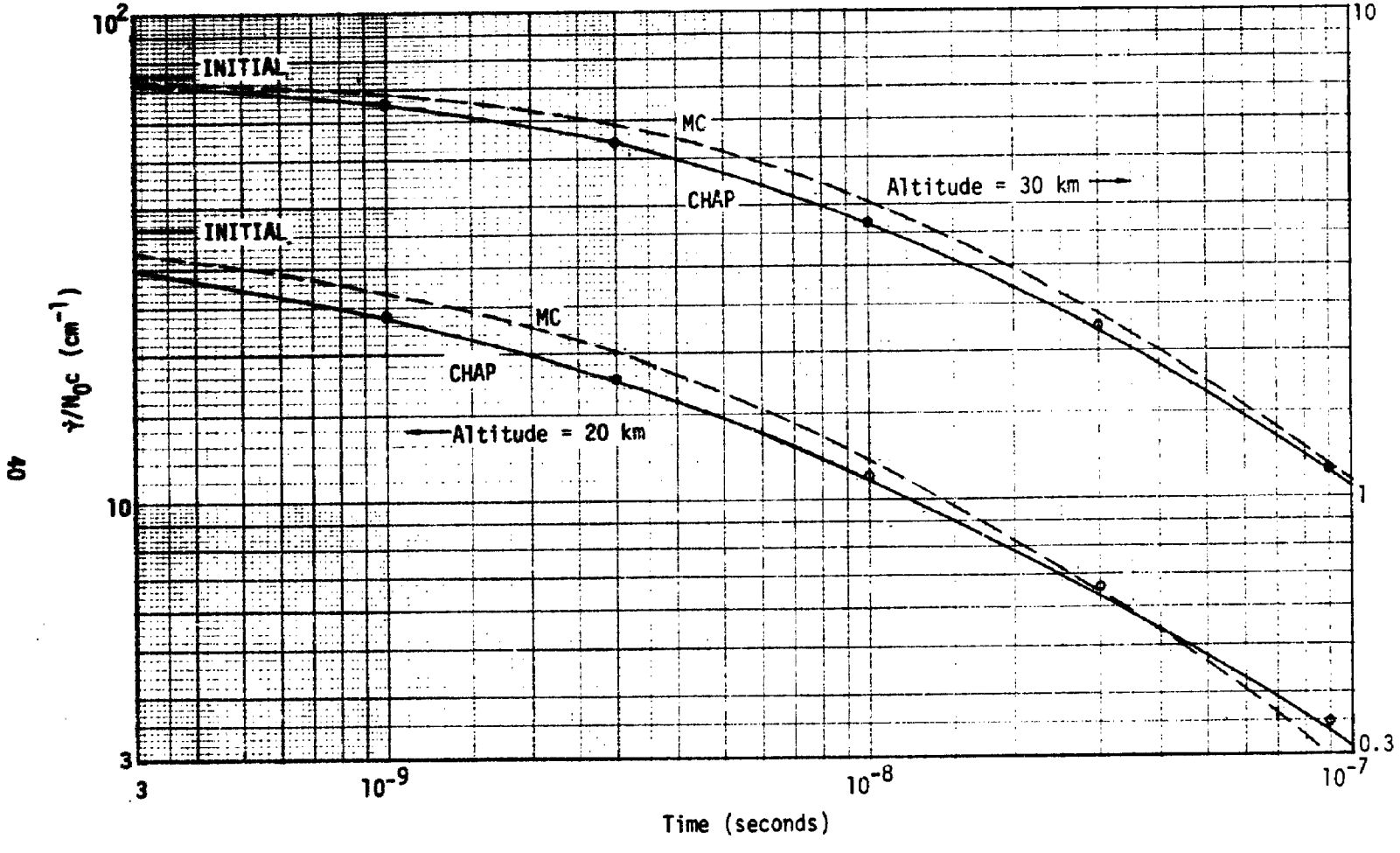

Figure 9. Ionization rate for E_γ = 1.6 MeV, B_y = 0.6 Gauss. Curve labels indicate: INITIAL, initial value; MC, Monte Carlo; CHAP, results from new obliquity factor method. Circles are points from old method.

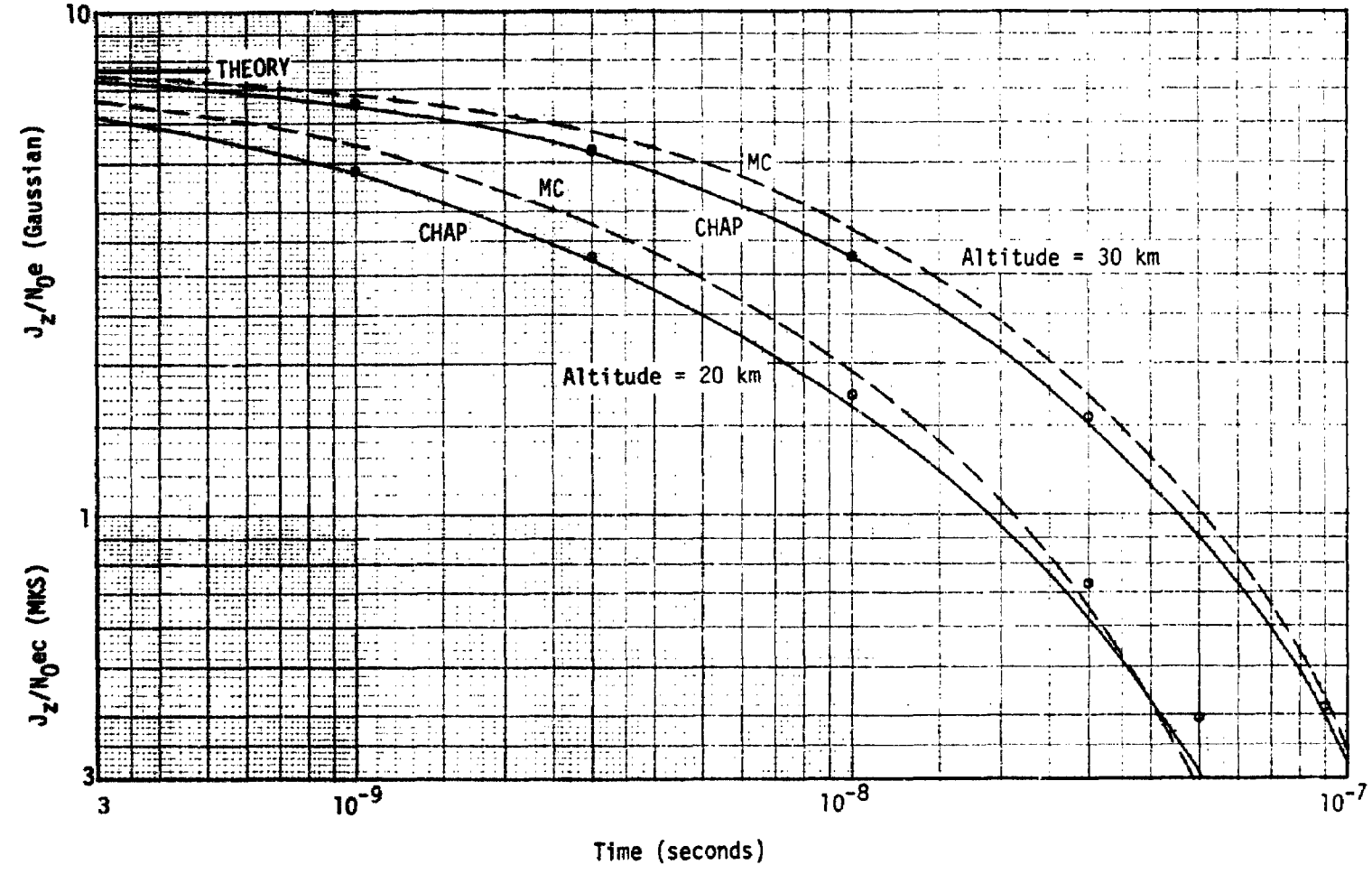

Figure 10. Radial current for E_γ = 1.6 MeV, B_y = 0.6 Gauss. Curve labels indicate: THEORY, theoretical initial value; MC, Monte Carlo; CHAP, new obliquity factor method. Circles are points from old method.

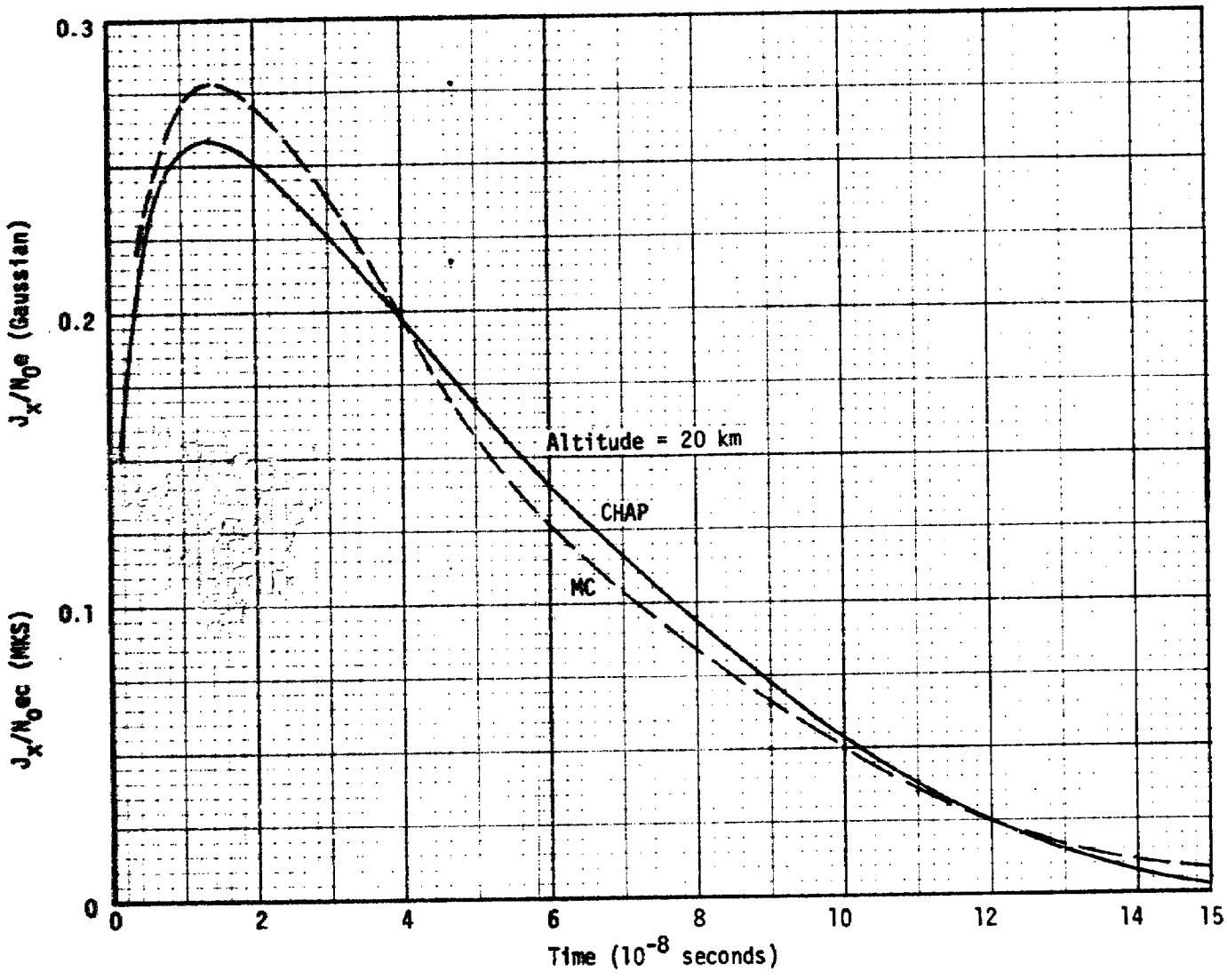

Figure 11. Transverse current for E_γ = 1.5 MeV, B_y = 0.56 Gauss. Curve labels indicate: MC, Monte Carlo by Knutson; CHAP, new obliquity factor method.

Carlo curves to the CHAP curves are nearly identical in the two figures. This indicates that our Monte Carlo results and those of Knutson and Morgan are very nearly identical, and supports the reliability of all of the calculations.

SECTION 10
COMPARISON WITH SOLLFREY'S RESULTS

In Figure 12 we compare Sollfrey's computed transverse currents with our Monte Carlo results at altitudes of 20 and 30 km. We see that there are substantial differences. Comparing with Figures 6 and 7, we see that the CHAP results are much closer to the Monte Carlo results than are Sollfrey's results. This is disappointing since we had hoped that Sollfrey's calculations would provide an accurate, independent check on the Compton currents.

Not having gone through Sollfrey's calculations in detail (they are quite lengthy), we can neither confirm them nor point to any errors. We do raise the question, however, as to whether the series, in terms of which his result is expressed, is convergent or only semiconvergent. In this connection, we point out that his first term J_0 is closer to our Monte Carlo results than is his sum $J_0 + J_1 + J_2$, and note that in his Figures 9a, b, c, the series does not appear to be converging, for J_2 is generally larger than J_1. It appears that if one more term were added, the result would be larger than the vacuum current and the theoretical initial slope at early times. In our view, these points raise serious doubt as to the accuracy of Sollfrey's results. We would like to see these questions resolved.

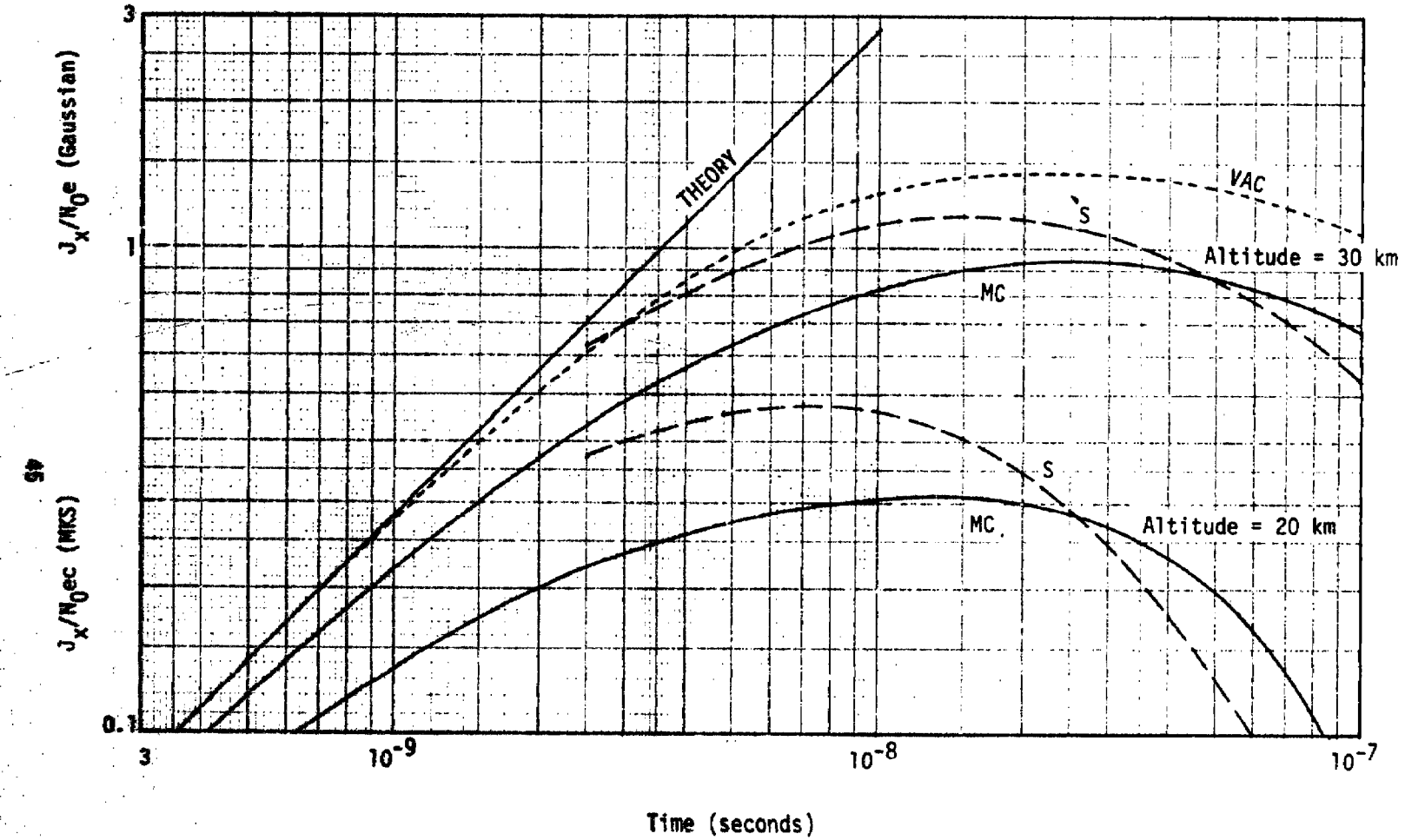

Figure 12. Transverse current for E_γ = 1.6 MeV, B_y = 0.6 Gauss. Curve labels indicate: THEORY, theoretical initial slope; VAC, zero air density; MC, Monte Carlo; S, Sollfrey's computed results.

SECTION 11
CONCLUSION

We have developed the theory of the Compton current in the presence of the geomagnetic field. We have derived analytically the initial value of the radial Compton current and the initial rate of rise of the transverse Compton current (which starts from zero initially). Neither of these values is affected by energy loss or scattering of the Compton electrons, and they serve as checks on numerical calculations. We have explained the approximate but fast method used in the CHAP code for calculating the Compton current, including the effects of energy loss and scattering. We have devised an accurate Monte Carlo calculation for the Compton current and have shown that it gives good agreement with experimental data on the transmission of electrons through aluminum foils. We have compared results from CHAP with those from our Monte Carlo, and have shown that CHAP results are within a few percent from the Monte Carlo results. Since CHAP errors in Compton current and ionization rate are in the same direction and about the same magnitude, the peak (saturated) electric field calculated by CHAP should be within 2 or 3 percent of the correct values. We have shown that our Monte Carlo results are nearly identical with similar results obtained by Knutson and Morgan in one case available to us.

We have compared Sollfrey's numerically computed Compton currents with our Monte Carlo results, and found discrepancies as large as 50 percent at important times. We have suggested that Sollfrey's series may not be convergent.

Sections 1 through 9 of this report are suitable for inclusion in a textbook on high-altitude EMP.

REFERENCES

1. Longmire, C. L., Close-In EM Effects Lectures X and IX, Los Alamos Scientific Laboratory, LAMS-3073, April 1964, unpublished.

2. Karzas, W. J., and R. Latter, Phys. Rev., Vol. 137B, pg. 1369, 1965.

3. Longley, H. J., and C. L. Longmire, Development of the CHAP EMP Code, DNA 3150T, MRC-R-3, Mission Research Corporation, January 1972, unpublished.

4. Longmire, C. L., and H. J. Longley, Improvements in the Treatment of Compton Current and Air Conductivity in EMP Problems, DNA 3192T, MRC-N-2, Mission Research Corporation, October 1971.

5. Longmire, C. L., and J. Koppel, Formative Time Lag of Secondary Ionization, MRC-R-88, Mission Research Corporation, January 1974.

6. Longley, H. J., and C. L. Longmire, Development of CHAP—A High-Altitude EMP Code, MRC-R-375, Mission Research Corporation, December 1977, unpublished.

7. Sollfrey, W., Analytic Theory of the Effects of Atmospheric Scattering on the Current and Ionization Produced by the Compton Electrons from High Altitude Nuclear Explosions, R-1973-AF, The RAND Corporation, October 1977.

8. Heitler, W., The Quantum Theory of Radiation, Oxford University Press, 1954.

9. Bethe, H. J., and J. Ashkin,"Passage of Radiations Through Matter," Experimental Physics, Vol. 1, E. Segre (ed.), John Wiley and Company, New York, 1953.

10. Moliere, G., Zeitschrift fur Naturforschung, Vol. 2a, 1947, p. 133, and Vol. 3a, 1948, p. 78.

11. Marshall, J. S., and A. G. Ward, Canadial Journal of Research, Vol. 15, Sec. A, 1937, p. 39.

12. Knutson, G. R., and J. F. Morgan, The Treatment of Electron Scattering and Approximate Methods Used for Specifying High-Altitude EMP Sources, EMP Theoretical Note 204, September 1973.

DISTRIBUTION LIST

DEPARTMENT OF DEFENSE

Assistant to the Secretary of Defense
Atomic Energy
ATTN: Executive Assistant

Defense Civil Preparedness Agency
Assistant Director for Research
ATTN: TS, AED

Defense Communication Engineer Center
ATTN: Code R720, C. Stansberry

Defense Communications Agency
ATTN: CCTC, C313
ATTN: CCTC, C312

Defense Documentation Center
Cameron Station
12 cy ATTN: TC

Defense Nuclear Agency
ATTN: DDST
4 cy ATTN: TITL

Interservice Nuclear Weapons School
ATTN: Document Control

Joint Strat. Tgt. Planning Staff
ATTN: JPST
ATTN: JSAS

Livermore Division, Field Command, DNA
Department of Defense
Lawrence Livermore Laboratory
ATTN: FCPRL

National Security Agency
Department of Defense
ATTN: R522
ATTN: S232, D. Vincent

Under Secretary of Defense for Rsch. & Engrg.
Department of Defense
ATTN: Strategic & Space Systems (OS)

DEPARTMENT OF THE ARMY

FRADCOM Technical Support Activity
Department of the Army
ATTN: DRSEL-TL-MD, G. Gaule
ATTN: DRSEL-TL-ME
ATTN: E. Hunter

Harry Diamond Laboratories
Department of the Army
ATTN: DELHD-RBA
ATTN: DELHD-EM
ATTN: W. Wyatt
2 cy ATTN: DELHD-RBC

U.S. Army Ballistic Research Labs
ATTN: DRXBR-AM, W. Van Antwerp

DEPARTMENT OF THE ARMY (Continued)

U.S. Army Comm-Elec. Engrg. Instal. Agency
ATTN: CCC-CED-SES

U.S. Army Electronics Rsch. & Dev. Command
U.S. Army Electronics Command
ATTN: DRCPM-ATC

U.S. Army Intelligence & Sec. Cmd.
Arlington Hall Station
ATTN: Technical Information Facility

DEPARTMENT OF THE NAVY

Office of Naval Research
ATTN: Code 427

Civil Engineering Laboratory
Naval Construction Battalion Center
ATTN: Code L08A

Naval Ocean Systems Center
ATTN: Code 015, C. Fletcher

Naval Research Laboratory
ATTN: Code 4104, E. Brancato
ATTN: Code 6623, R. Statler

Naval Surface Weapons Center
Dahlgren Laboratory
ATTN: Code DF-56

Naval Weapons Evaluation Facility
ATTN: Code AT-6

Strategic Systems Project Office
Department of the Navy
ATTN: NSP-230, D. Gold
ATTN: NSP-2342, R. Coleman
ATTN: NSP-27334

DEPARTMENT OF THE AIR FORCE

AF Weapons Laboratory, AFSC
ATTN: NTN
ATTN: NXS
ATTN: ELP. W. Page

Air Force Technical Applications Center
ATTN: TFS, M. Schneider

Aeronautical Systems Division, AFSC
ATTN: ASD-YH-EX

Foreign Technology Division, AFSC
ATTN: NICD, Library

Sacramento Air Logistics Center
Department of the Air Force
ATTN: MMSREM, F. Spear
ATTN: MMCRS, N. Palmastro
ATTN: MMIRA, J. Demes

DEPARTMENT OF ENERGY

Department of Energy
Albuquerque Operations Office
ATTN: Operational Safety Div.

Lawrence Livermore Laboratory
ATTN: Doc. Con. for D. Meeker, L-545
ATTN: Doc. Con. for J. Miller, L-156

Los Alamos Scientific Laboratory
ATTN: Doc. Con. for B. Noel

Sandia Laboratories
ATTN: Doc. Con. for E. Hartman
ATTN: Doc. Con. for C. Vittitoe

DEPARTMENT OF DEFENSE CONTRACTORS

Aerospace Corporation
ATTN: C. Greenhow

Bendix Corporation
Research Laboratories Division
ATTN: M. Frank

Bendix Corporation
ATTN: Dept. 6401

The Boeing Company
ATTN: H. Wicklein

Computer Sciences Corporation
ATTN: R. Dickhaut

Dikewood Industries, Inc.
ATTN: K. Lee

Fairchild Camera and Instrument Corporation
ATTN: D. Myers

Franklin Institute
ATTN: R. Thompson

General Electric Company
Aerospace Electronics Systems
ATTN: C. Hewison

General Electric Company
ATTN: Technical Library

General Electric Company-TEMPO
Alexandria Office
ATTN: DASIAC

General Research Corporation
Santa Barbara Division
3 cy ATTN: Technical Information Office

Georgia Institute of Technology
Office of Contract Administration
ATTN: Rsch. & Security Coordinator for H. Denny

GTE Sylvania, Inc.
Electronics Systems Grp.-Eastern Div.
ATTN: L. Blaisdell

Hazeltine Corporation
ATTN: M. Waite

DEPARTMENT OF DEFENSE CONTRACTORS (Continued)

Hughes Aircraft Company
ATTN: K. Walker

IIT Research Institute
Electromag. Compatability Anal. Ctr.
ATTN: ACOAT

International Tel. & Telegraph Corporation
ATTN: A. Richardson

Kaman Sciences Corporation
ATTN: J. Lubell

Lockheed Missiles & Space Company, Inc.
ATTN: B. Kimura
ATTN: M. Bernstein

Mission Research Corporation
ATTN: C. Longmire
5 cy ATTN: Technical Library

Northrop Corporation
Electronic Division
ATTN: Rad. Effects Grp., B. Ahlport

RCA Corporation
Camden Complex
ATTN: R. Rostrom

Rockwell International Corporation
ATTN: N. Rudie

Sanders Associates, Inc.
ATTN: R. Despathy, Sr.

Science Applications, Inc.
Huntsville Division
ATTN: N. Byrn

The Rand Corporation
ATTN: W. Sollfrey

R&D Associates
ATTN: M. Grover
ATTN: J. Bombardt

Sperry Rand Corporation
Sperry Microwave Electronics
ATTN: M. Cort

Spire Corporation
ATTN: J. Uglum

Systems, Science & Software, Inc.
ATTN: A. Wilson

TRW Defense & Space Sys. Group
ATTN: H. Holloway
ATTN: R. Plebuch

United Technologies Corporation
Hamilton Standard Division
ATTN: Chief, Elec. Design